RELAP5 Mod 3.2.2 Gamma Results for the Palisades 1D Downcomer Sensitivity Study

William Arcieri[1]
C. Don Fletcher[1]
David Bessette[2]

[1]ISL, Inc.
11140 Rockville Pike
Rockville, MD 20852

[2]U.S. Nuclear Regulatory Commission
Office of Nuclear Regulatory Research
Washington, D.C. 20555-0001

August 31, 2004

Prepared for

U.S. Nuclear Regulatory Commission
Office of Nuclear Regulatory Research
Washington, D.C. 20555-0001

Table of Contents

List of Figures

List of Tables

1. Introduction

As part of the Pressurized Thermal Shock (PTS) Rebaselining Project, a Peer Review Group (PRG) was formed to provide review and comments on all phases of the PTS Rebaselining Project. Among the issues raised by the PRG was the mixed convection heat transfer correlations used to determine the heat transfer coefficient between the fluid and downcomer wall. Specifically, the PRG was concerned that the RELAP5 heat transfer coefficient values may be too low. The heat transfer coefficient used in RELAP5/MOD 3.2.2 Gamma is computed as the maximum of the forced convection, laminar convection, and natural convection values. The correlations used are by Dittus-Boelter, Kays, and Churchill-Chu. For parallel plates, the Petukhov correlation is used in place of Dittus-Boelter correlation and the Elenbass correlation is used instead of Churchill-Chu correlation [Ref. 1]. The PRG proposed the use of a multiplier on the heat transfer correlation based on work by Swanson and Catton [Ref. 2]. This work was reviewed and incorporated into the ORNL ANS Interphase model in RELAP5/Mod 3.2.2 gamma. This model is based on parallel plates and uses the Petukhov heat transfer correlation as described by Shumway [Ref. 3]. Additional work is being done to better integrate the Swanson-Catton multiplier into the Petukhov heat transfer correlation used in RELAP5 and further sensitivity cases are planned once the modifications are completed.

Another issue that emerged during the course of the peer review was the number of nodes used in the RELAP5 heat structures that are used to represent components such as the reactor vessel. Typically, the number of nodes used in RELAP5 models ranges from 8 to 15 nodes. The Palisades model used 8 nodes. As part of the sensitivity studies, the number of nodes in the Palisades model was increased from 8 to 80.

A set of sensitivity runs were made to evaluate the impact of heat transfer coefficient and vessel wall noding on RELAP5 predictions of downcomer fluid temperature, primary system pressure. A one-dimensional downcomer model based on the Palisades plant model described in the PTS Results Report [Ref. 4] was utilized in these sensitivity runs. Details on the model used, the sensitivity case defined, and the results of the sensitivity runs are presented in the following sections.

2. Palisades 1D Model Description and RELAP5 Code Changes

The Palisades PTS transients were analyzed using the two-dimensional downcomer model described in Section 2.3 of the PTS Results Report. This model utilized six azimuthal sectors around the circumference of the downcomer. This noding was used to capture the azimuthal variation in temperature and flow conditions in the downcomer. However, it was found that significant flow circulations may be predicted in some of the transients, principally those involving a LOCA, that were deemed to be unrealistic. These circulations can affect heat transfer coefficient predictions since these predictions are based on fluid velocity which is affected by the flow circulation. To eliminate the impact of flow circulation on heat transfer coefficient, a one dimensional downcomer model was used.

Figure 2-1 presents the vessel model used in the Palisades 1D sensitivity study. In developing the 2D downcomer model, the downcomer geometry was partitioned into six equal sectors with flow areas being set to 1/6 of the total. This process was basically reversed in developing the 1D model. Referring to Figure 2.3-1 of the PTS Results Report, downcomer sectors represented by components 500 to 506 were combined into a single component 500. Similarly, sectors 506 to 511 were recombined into a single sector 506. In both instances, the flow area was increased by a factor of 6. Multiple junction components 512, 513, and 514 were deleted, eliminating the cross flow connections. Multiple junctions used to connect various sections of the downcomer in the axial direction were replaced by single junctions and the flow area was increased by a factor of 6. All cold leg connections were connected to component 500020003.

Heat structure modifications were also made consistent with the changes in the hydrodynamic components. The heat structure representing the lower reactor vessel wall that interacts with component 500 (5701) was modified to be consistent with the changes made to that component. The number of heat structures was reduced from 36 in the 2D model to 6. The surface area entry values for the interior (downcomer) and exterior surfaces were increased by a factor of 6.

The heat structure representing the upper reactor vessel wall that interacts with component 506 (5702) was modified to be consistent with the changes made to that component. The number of heat structures was reduced from 6 to 1. The surface area entry values for the interior (downcomer) and exterior surfaces were increased by a factor of 6. Similarly, the heat structure representing the core barrel that interacts with component 500 (5051) was modified to be consistent with the changes made to that component. The number of heat structures was reduced from 37 to 7. The surface area entry values for the interior (downcomer) and exterior surfaces were increased by a factor of 6.

The vessel wall thickness was adjusted to agree with the thickness used in Favor. The minimum wall thickness is 21.6 cm (8.5 in) plus a nominal cladding thickness of 0.635 cm (0.25 in) cladding. For the upper part of the vessel wall, the minimum wall thickness is 27.31 cm (10.75 in) below the flange plus 0.25 inch clad, which is thicker to accept the bolts for the vessel head. The inner vessel radius is 218.4 cm (86 in) which corresponds to 436.8 cm (172 in) diameter.

Other changes to the model include controller changes reflecting changes to the downcomer nodalization and calculation of 1, 5, and 10 second running averages. Expanded plot variables were also added to the model to obtain interior downcomer wall node temperature and other parameters of interest. Modifications where the number of nodes in the downcomer wall was increased from 8 to 80 nodes were also included.

As part of the sensitivity calculations using the Swanson-Catton multiplier on heat transfer coefficient, the ORNL ANS Interphase model in RELAP5 was modified to incorporate the Swanson-Catton multiplier. Note that the Petukhov correlation is used in the ORNL ANS Interphase model. In addition, the Elenblaas equation for parallel plates was incorporated into RELAP5 to avoid issues with obtaining unrealistically large heat transfer coefficients using this model. With these changes, the code would then use the Swanson-Catton multiplier in the application of the ORNL ANS Interphase model to a RELAP5 analysis.

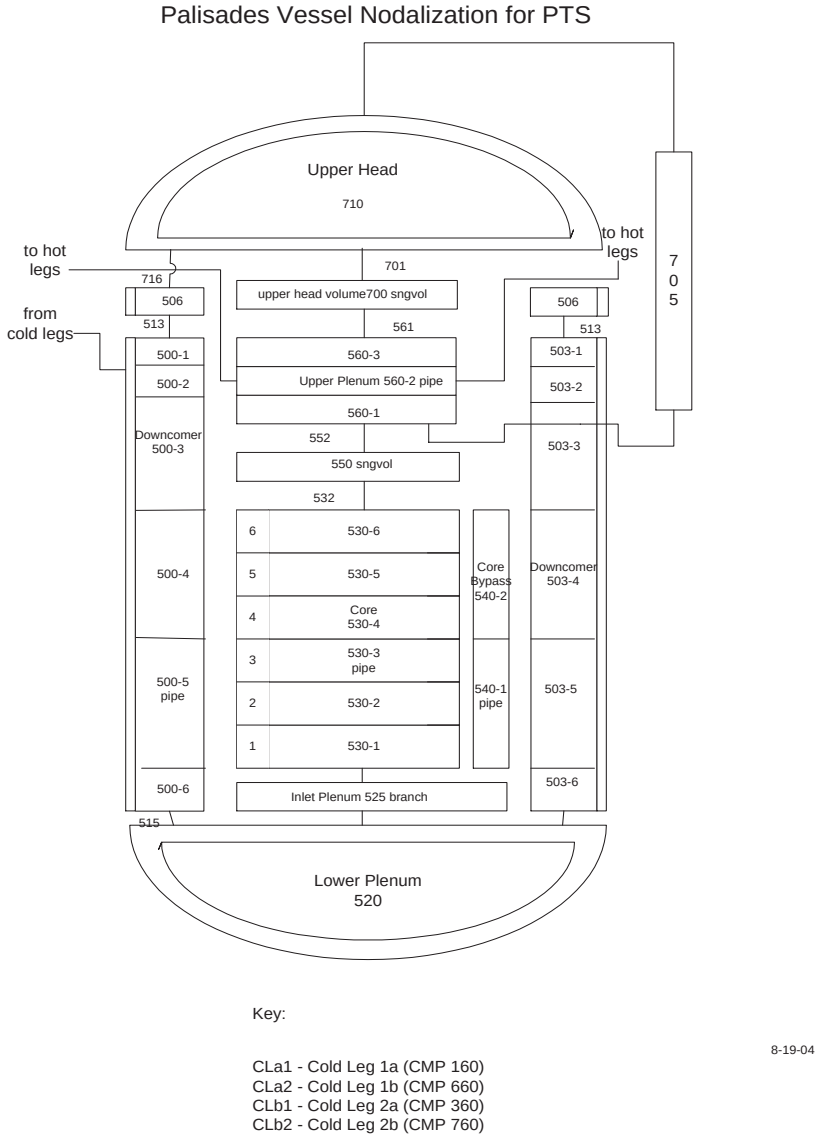

Figure 2-1: Palisades 1D Downcomer Vessel Model

In addition to the RELAP5 coding changes, input modifications are required to invoke the ORNL ANS Interphase model. The geometry type for the downcomer is changed from a pipe to an annulus and the volume control flag is set to invoke the ORNL ANS Interphase model in the affected component volumes. Also, the gap and the span of the downcomer node needs to be specified. In this case, the gap is the distance between the downcomer wall and the outside of the core barrel. The span is the circumference of the core barrel. The values used are 0.8545 ft for the gap and 39.66 ft for the span (circumference) of the core barrel. Heat structures that interface with the downcomer were also changed to use the ORNL ANS Interphase model at the structure boundary.

3. Cases Analyzed

Sensitivity cases that were analyzed were derived from the list of transients presented in Table 1. This list constitutes the transients that contribute 1 percent or more to the risk of reactor vessel failure at Palisades due to a PTS event (as of October 2003).

Table 1
Palisades Cases Used for Sensitivity Study

Case	System Failure	Operator Action	HZP
19	Reactor trip with 1 stuck-open ADV on SG-A.	None. Operator does not throttle HPI.	Yes
40	40.64 cm (16 in) hot leg break. Containment sump recirculation included in the analysis.	None. Operator does not throttle HPI.	No
52	Reactor trip with 1 stuck-open ADV on SG-A. Failure of both MSIVs (SG-A and SG-B) to close.	Operator does not isolate AFW on affected SG. Normal AFW flow assumed (200 gpm). Operator does not throttle HPI.	Yes
54	Main steam line break with failure of both MSIVs to close. Break assumed to be inside containment causing containment spray actuation.	Operator does not isolate AFW on affected SG. Operator does not throttle HPI.	No
55	Turbine/reactor trip with 2 stuck-open ADVs on SG-A combined with controller failure resulting in the flow from two AFW pumps into affected steam generator.	Operator starts second AFW pump.	No

Table 1 Palisades Cases Used for Sensitivity Study			
Case	System Failure	Operator Action	HZP
58	10.16 cm (4 in) cold leg break. Winter conditions assumed (HPI and LPI injection temp = 40 F, Accumulator temp = 60 F)	None. Operator does not throttle HPI.	No
59	10.16 cm (4 in) cold leg break. Summer conditions assumed (HPI and LPI injection temp = 100 F, Accumulator temp = 90 F)	None. Operator does not throttle HPI.	No
60	5.08 cm (2 in) surge line break. Winter conditions assumed (HPI and LPI injection temp = 40 F, Accumulator temp = 60 F)	None. Operator does not throttle HPI.	No
62	20.32 cm (8 in) cold leg break. Winter conditions assumed (HPI and LPI injection temp = 40 F, Accumulator temp = 60 F)	None. Operator does not throttle HPI.	No
63	14.37 cm (5.656 in) cold leg break. Winter conditions assumed (HPI and LPI injection temp = 40 F, Accumulator temp = 60 F)	None. Operator does not throttle HPI.	No
64	10.16 cm (4 in) surge line break. Summer conditions assumed (HPI and LPI injection temp = 100 F, Accumulator temp = 90 F)	None. Operator does not throttle HPI.	No
65	One stuck-open pressurizer SRV that recloses at 6000 sec after initiation. Containment spray is assumed not to actuate.	None. Operator does not throttle HPI.	Yes
Note: HZP is an abbreviation for hot zero power.			

Variations on the sensitivity runs for each of the transients listed in Table 1 are presented in Table 2. A total of 12 variations are applied to each transient in the Table 1 transient set, resulting in a total of 144 sensitivity cases. Running averages of 1, 5, and 10 seconds on the downcomer fluid temperature, primary system pressure and downcomer fluid to vessel wall heat transfer coefficient are calculated in each run and output at a 1 second output interval. Note that the output interval in the original Palisades analysis was 15 seconds. Hot full power and hot zero power steady state runs were performed and applied as appropriate to each transient to ensure proper initial conditions.

In two of the variations listed in Table 2, multipliers of 0.7 and 1.3 were applied to the cases where the ORNL ANS Interphase (Petukhov) model is applied. The basis for this range of multipliers is that the uncertainty in the heat transfer coefficient predicted by the Dittus-Boelter correlation is 30%.

Table 2
Summary of Sensitivity Run Variations

Variation Number	Downcomer Noding	# of Downcomer Wall Nodes Used	Running Average Time Value (s)	Heat Transfer Coefficient Model	Heat Transfer Coefficient Multiplier
1	2D	8	none	Dittus-Boelter	1.0
2	1D	8	none	Dittus-Boelter	1.0
3	1D	8	1	Dittus-Boelter	1.0
4	1D	8	5	Dittus-Boelter	1.0
5	1D	8	10	Dittus-Boelter	1.0
6	1D	80	none	Dittus-Boelter	1.0
7	1D	80	1	Dittus-Boelter	1.0
8	1D	80	5	Dittus-Boelter	1.0
9	1D	80	10	Dittus-Boelter	1.0
10	1D	80	10	Petukhov	1.0
11	1D	80	10	Petukhov	0.7
12	1D	80	10	Petukhov	1.3
Note that the output interval for all sensitivity studies listed in this table is 1 second.					

4. Results

A summary of the key RELAP5 results for the sensitivity cases is presented in this section. Because of the large number of cases, a CDROM with a set of plots that show plots of downcomer fluid temperature, primary system pressure and downcomer fluid to vessel wall heat transfer along with plots of various system parameters is included with this letter report. This CDROM contains system plots as well as plots of the average downcomer fluid temperature and average downcomer fluid to wall heat transfer coefficient for each of the sensitivity cases presented in this report.

The results from the original Palisades analysis discussed in the PTS Results Report (Ref. 4) are compared to Variations 1 and 2 listed in Table 2. The only difference between the Results Report analysis and the Variation 1 analysis is the output interval and, essentially there is no difference (mean difference is < 0.1 K (0.2°F)). These results are found in the Original_1s subdirectory in the SystemPlots directory in the attached CDROM.

4.1 2D Downcomer Model Results vs. 1D Downcomer Model Results

Figures 4-1 through 4-12 present a summary of the average downcomer temperature difference between the 2D downcomer results (Original_1s) and the 1D downcomer results for each of the transients listed in Table 1. Variations 1 through 5 listed in Table 2 are shown for each transient on these figures. Detailed plots are found in the 1D subdirectory in the SystemPlots directory ion the attached CDROM.

Changing the downcomer model from a 2D to a 1D nodalization does not have a strong impact on average downcomer temperature results for those transients involving secondary side failures such as a stuck open atmospheric dump valves or a main steam line break. These transients include Cases 19, 52, 54 and 55. In Cases 19, 52, and 55, at least two of the reactor coolant pumps remain running which results in turbulent flow and mixing in the downcomer. Also, no significant differences are seen in the primary system pressure or in the timing of high pressure injection (HPI) initiation and flow rate. The average temperature difference is less than about 2 K (4°F). In Case 54, the reactor coolant pumps are tripped since the main steam line break is assumed to occur in containment. However, turbulent flow and mixing in the downcomer occurs because of natural circulation through the loops due to continued heat removal in the steam generators. The average temperature difference is about 8 K (15°F) for Case 54.

The cases involving a loss of coolant accident (LOCA) or a stuck open primary system relief valve show varying degrees of change on the downcomer temperature due to the 2D to 1D modeling change. The average downcomer temperature difference for the stuck open primary system safety valve, Case 65, is about 7 K (12°F). There is a slightly lower primary system pressure after 2000 sec (see page 5 of the case065_1D.pdf file in the 1D directory). This pressure difference results in a slightly higher HPI flow (page 21 of the case065_1D.pdf file) which causes the downcomer temperature difference. On the opposite end of the break size spectrum is Case 40, which is a 40.64 cm (16 in) hot leg break. The results of Case 40 shows an average downcomer temperature difference of about 4 K (7°F), which is relatively small. This

difference is attributed to the rapid primary system depressurization due to the size of the break which causes almost immediate actuation of the safety injection tanks and also the high and low pressure injection systems.

The LOCAs with break sizes between the stuck open primary system relief valve and the large 40.64 cm (16 in) hot leg break show the most difference, which is not surprising given the various break sizes, break locations, and injection water temperatures analyzed. Starting with the 20.32 cm (8 in) cold leg break shown in Figure 4-10, the average downcomer temperature is generally higher in the 1D downcomer model results. This difference is due to a slightly higher primary system pressure prediction in the 1D case, resulting in lower emergency core cooling system (ECCS) injection, particularly low pressure injection (pages 4 and 22 of the case062_1D.pdf file). Note that this break is of sufficient size so that the high and low pressure injection systems will be operating at essentially runout conditions, so that the downcomer temperature is governed largely by the ECCS flow rate.

The remaining transients (Cases 58, 59, 60, 63, and 64) are of a break size (between 5.08 cm (2 in) and 14.37 cm (5.656 in)) where the rate of ECCS injection tends to be limited by the break size (sheets 18 and 24 of the aforementioned cases in the 1D directory). The average downcomer temperature in these cases is most affected by the change in downcomer modeling, particularly the cold leg break cases.

One reason for the difference in downcomer temperature in the cold leg break cases is the degree of mixing that occurs in the downcomer. In the 2D downcomer model, allowing flow in the cross-flow direction tends to enhance flow in the axial direction on average so that more of the warm downcomer water is mixed with the ECCS injection water. This mixing effect tends to occur throughout the downcomer so that water in the lower plenum (and the core) can also contribute to warming the downcomer. This effect is seen by comparing the temperature results for Cases 59 and 64 which are both 10.16 cm (4 in) breaks with equivalent ECCS injection temperatures but with the break location in the cold leg or surge line, respectively. The average downcomer temperature difference is somewhat greater in the cold leg break case (Case 59) compared to the surge line break case (Case 64). In both cases, the 1D downcomer temperature results tend to be somewhat lower compared to the original 2D results.

Downcomer temperature differences are also seen in breaks in the surge line. In these cases, allowing flow in the cross-flow direction will enhance flow in the axial direction. However, since the surge line break results in a “flow-through” situation, there is sufficient axial flow so that the difference in mixing in the downcomer due to 2D vs. 1D modeling differences is not as great as in the cold leg break cases.

Plots of running averages are shown in Figures 4-1 to 4-12. As expected, there is little to no difference in the results between the non-averaged and the average data, although the averaged data is a little smoother.

Plots of the average downcomer fluid to wall heat transfer coefficient are shown in the avgHTC_1D.pdf file in the 1D directory in the attached CDROM.

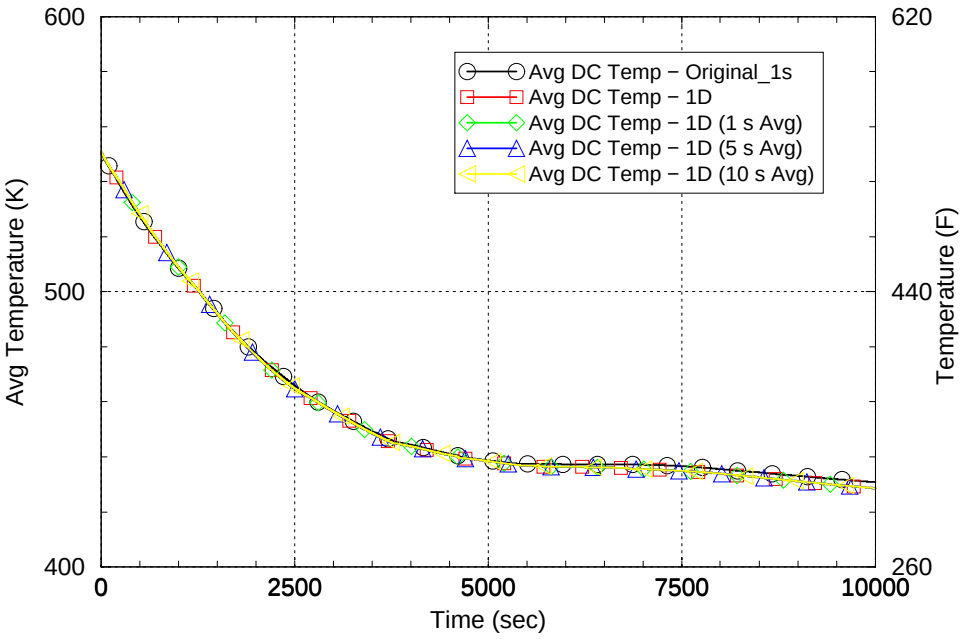

Figure 4-1: Case 19 Avg. Downcomer Temperature (Original vs 1D)

.

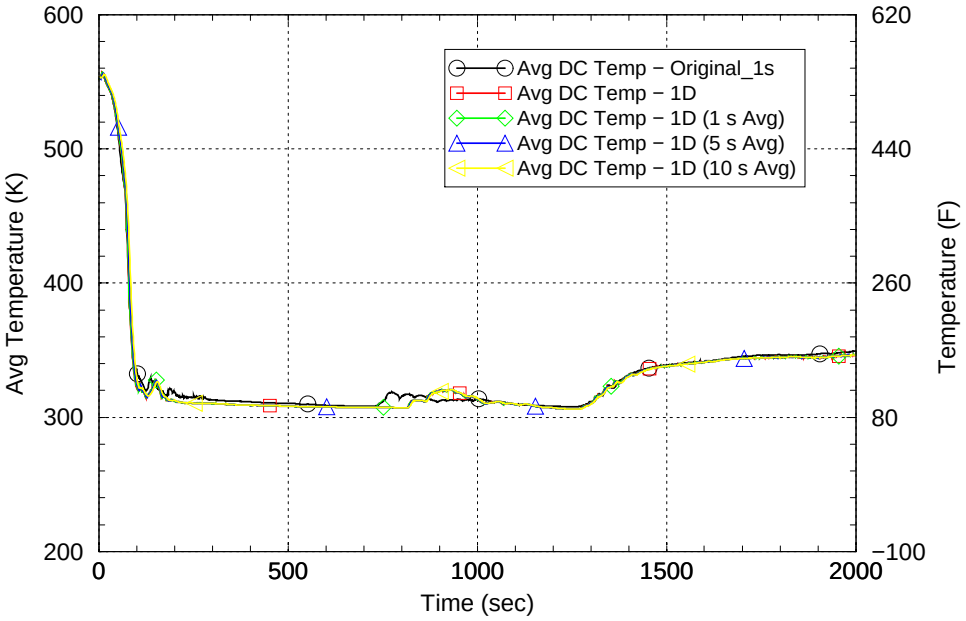

Figure 4-2: Case 40 Avg. Downcomer Temperature (Original vs 1D)

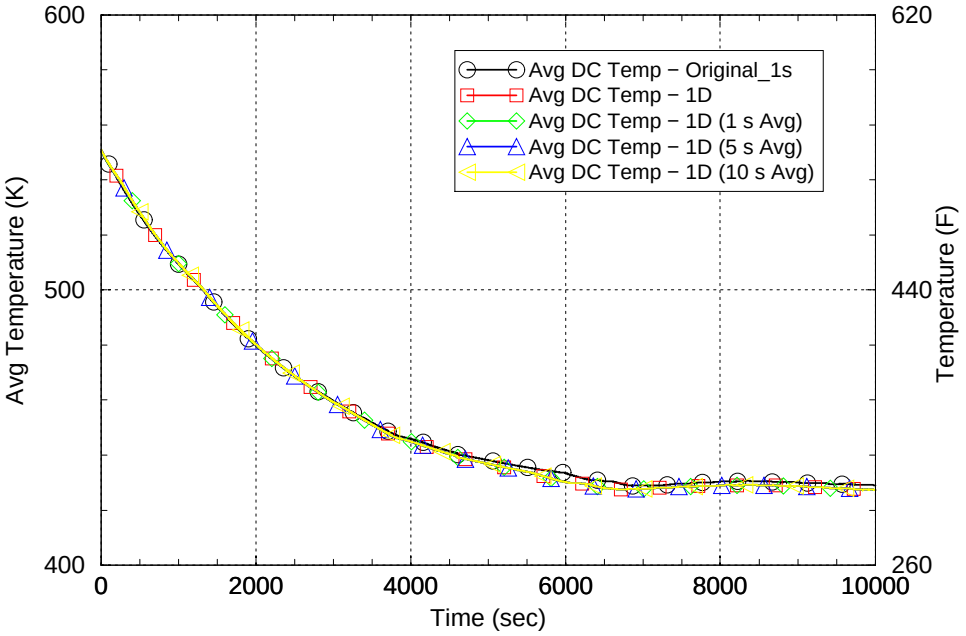

Figure 4-3: Case 52 Avg. Downcomer Temperature (Original vs 1D)

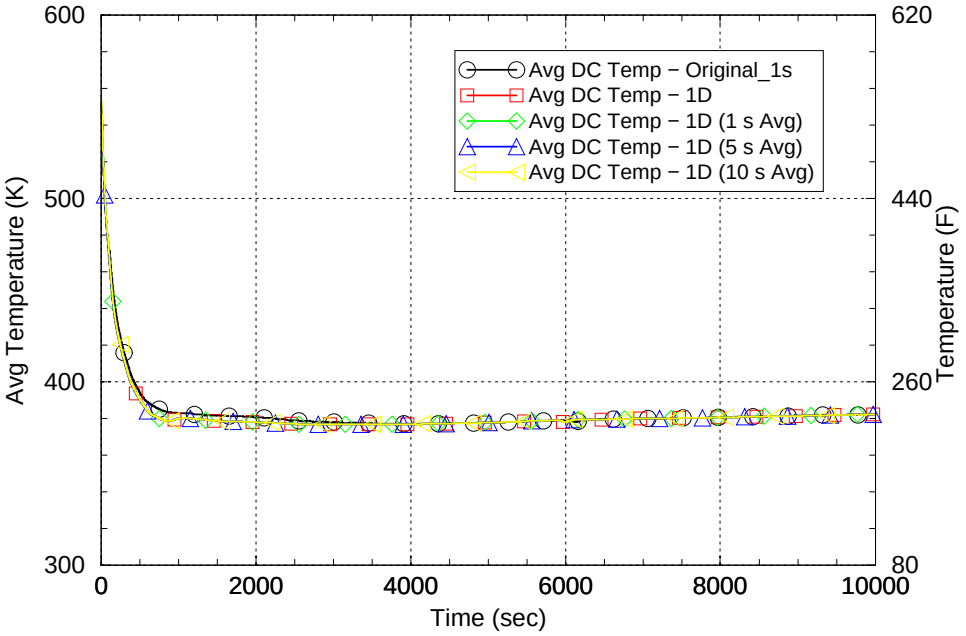

Figure 4-4: Case 54 Avg. Downcomer Temperature (Original vs 1D)

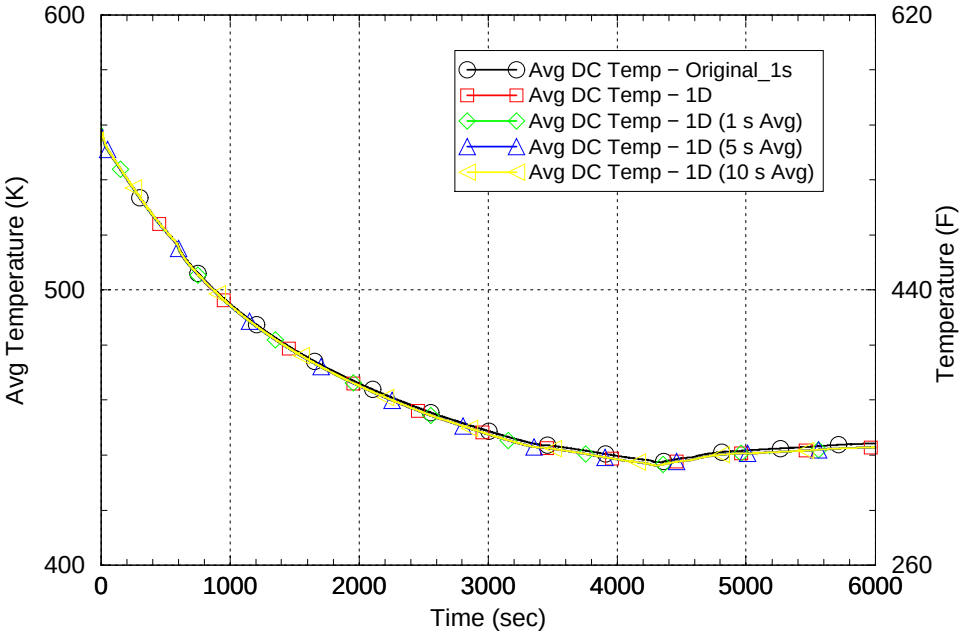

Figure 4-5: Case 55 Avg. Downcomer Temperature (Original vs 1D)

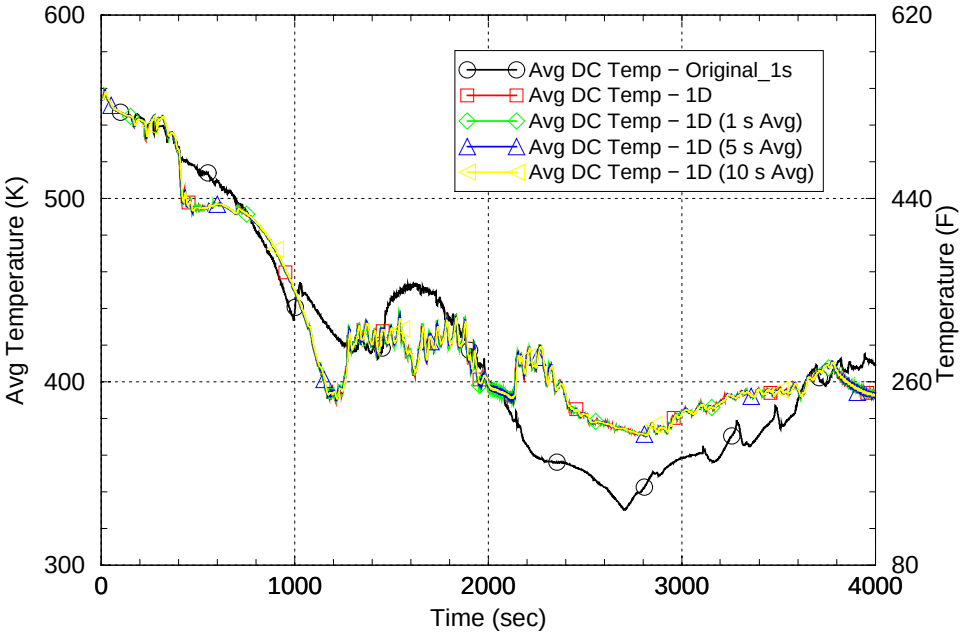

Figure 4-6: Case 58 Avg. Downcomer Temperature (Original vs 1D)

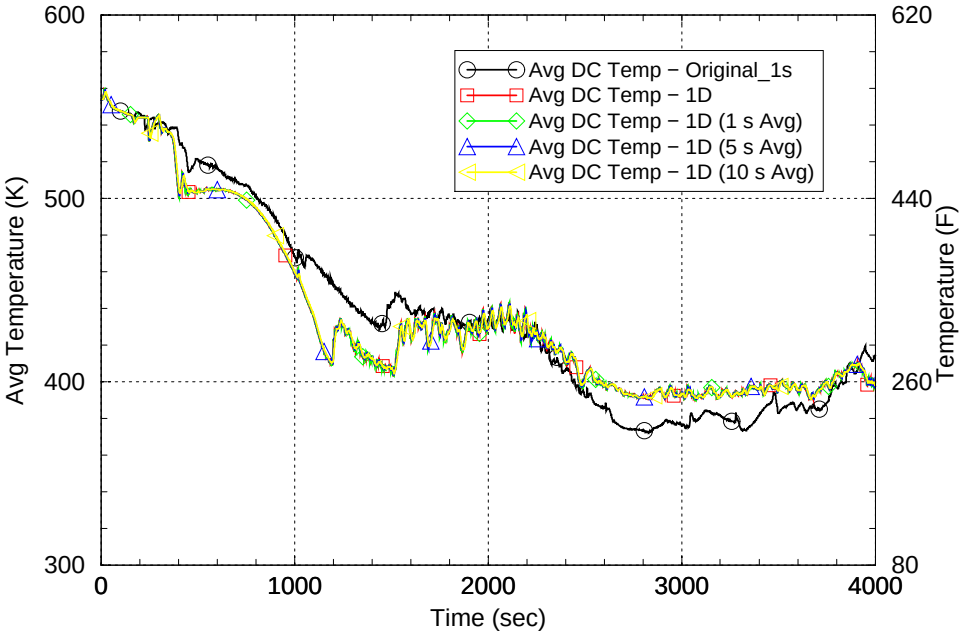

Figure 4-7: Case 59 Avg. Downcomer Temperature (Original vs 1D)

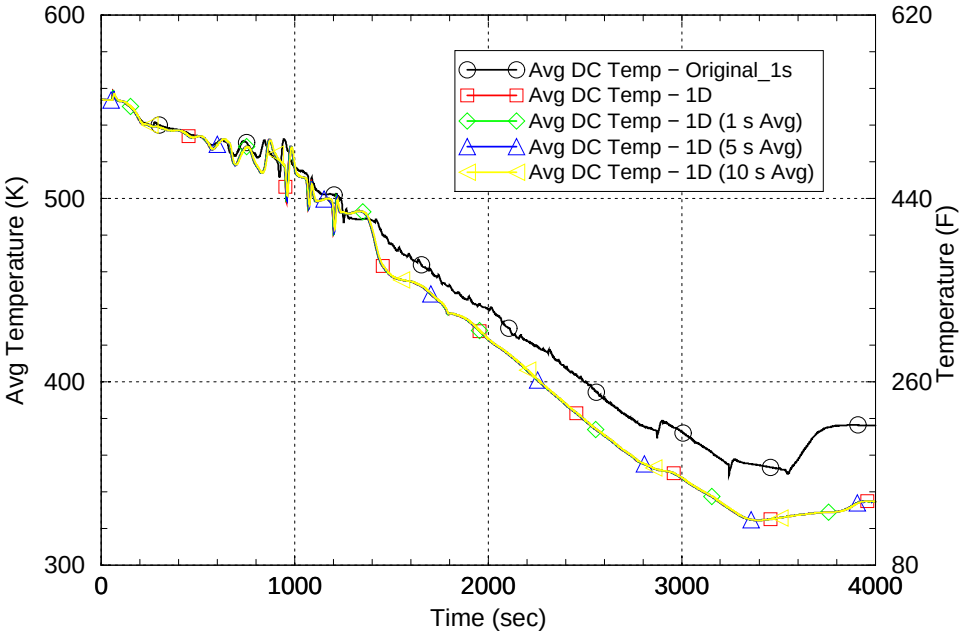

Figure 4-8: Case 60 Avg. Downcomer Temperature (Original vs 1D)

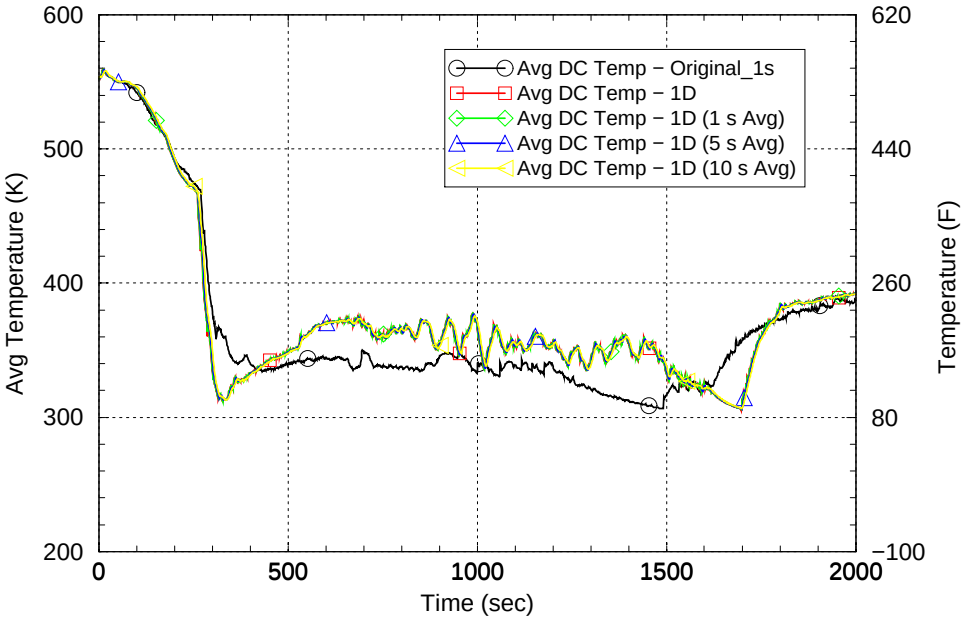

Figure 4-9: Case 62 Avg. Downcomer Temperature (Original vs 1D)

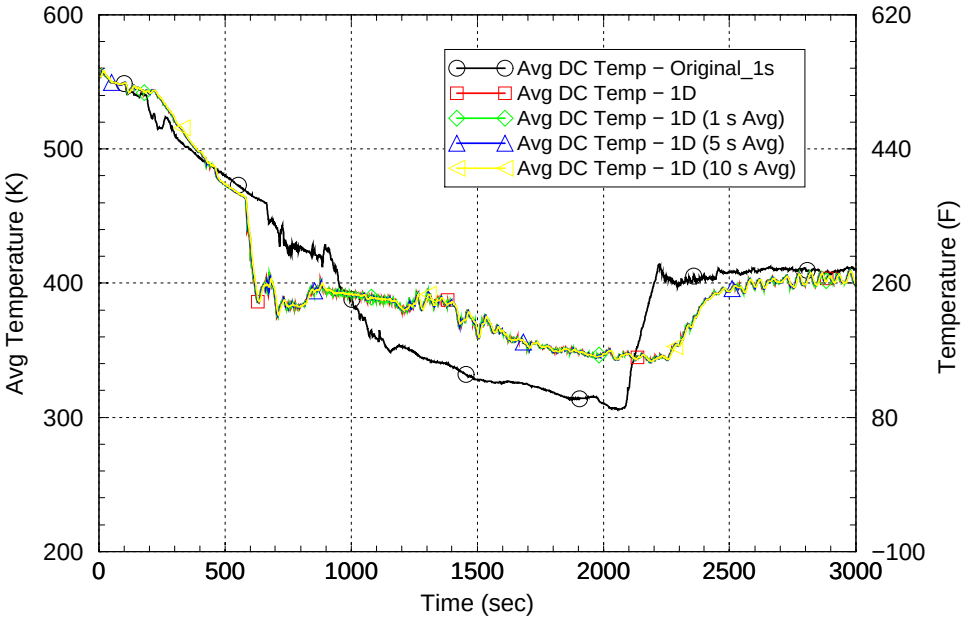

Figure 4-10: Case 63 Avg. Downcomer Temperature (Original vs 1D)

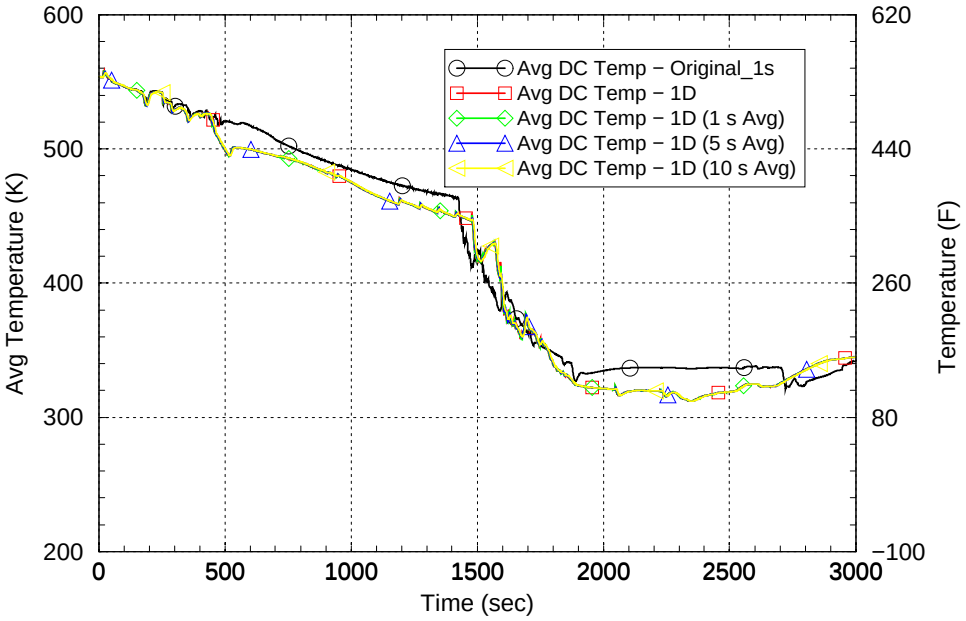

Figure 4-11: Case 64 Avg. Downcomer Temperature (Original vs 1D)

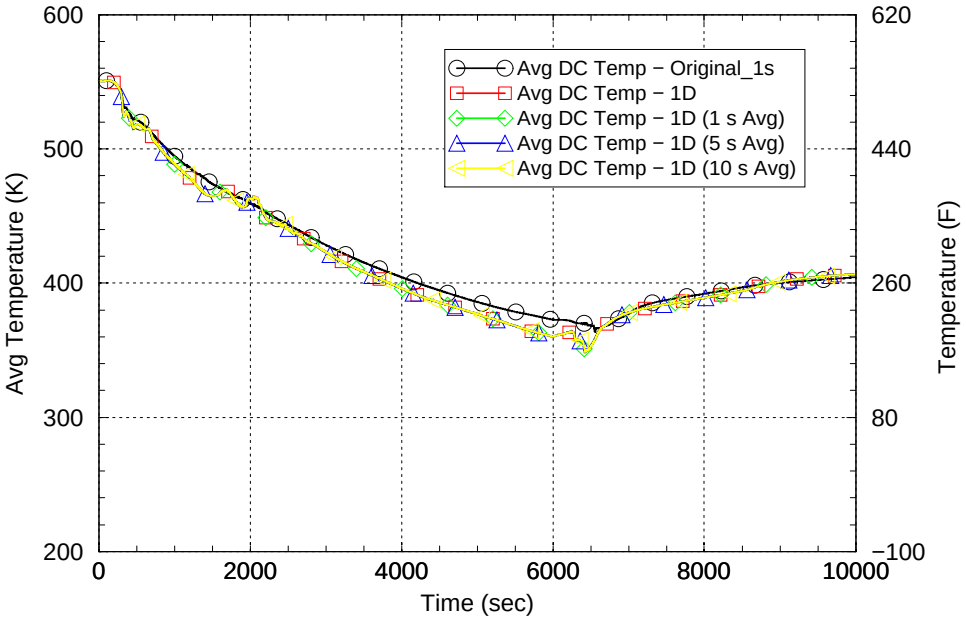

Figure 4-12: Case 65 Avg. Downcomer Temperature (Original vs 1D)

4.2 1D Model Results with 80 Nodes in Downcomer Wall

Figures 4-13 through 4-24 present a summary of the average downcomer temperature difference between the 1D downcomer results with 8 nodes in the vessel wall and the 1D downcomer results using 80 nodes in the vessel wall for each of the transients listed in Table 1. Variations 1 and 6 are compared in these figures. The running average cases listed in Variations 7 through 9 are not included as these results basically overlay the results of Variation 6. Detailed plots of the 1D downcomer results are found in the 1D_80pt directory on the attached CDROM.

Increasing the number of nodes in the downcomer vessel wall from 8 nodes to 80 nodes does not have a strong impact on the average downcomer temperature results for most of the transients analyzed in this sensitivity study. Case 58, a 10.16 cm (4 in) cold leg break with winter conditions assumed, shows the largest difference of any of the transients. The largest difference occurs at about 2200 seconds and is due to differences in the low pressure injection rate (page 22 in the case058_1D_80pt.pdf file in the 1D_80pt directory). The number of nodes used in the vessel wall has some influence on downcomer fluid velocity as seen from looking at the results for the average downcomer fluid to wall heat transfer coefficient in the range of 500 to 1000 seconds after initiation (see page 6 of the avgHTC_1D_80pt.PDF file in the 1D_80pt directory). This difference affects the average downcomer fluid temperature during this time period.

The average downcomer fluid temperature results for Case 59, a 10.16 cm (4 in) cold leg break with summer conditions assumed, shows some differences in the time period of 1100 to 1400 seconds after initiation. The system plots show differences in the void behavior in the cold legs during this period (pages 27 to 30 of case059_1D_80pt.pdf) which affects the break flow (page 18 of file case059_1D_80pt.pdf) and causes the difference in temperature. Differences later in the transient (1500 to 1800 seconds after initiation) are also seen in the results for Case 62, an 20.32 cm (8 in) cold leg break with winter conditions assumed. These differences are also tied to the void behavior in the cold leg which affects the break flow (see pages 18 and 27 to 30 of file case062_1D_80pt.pdf).

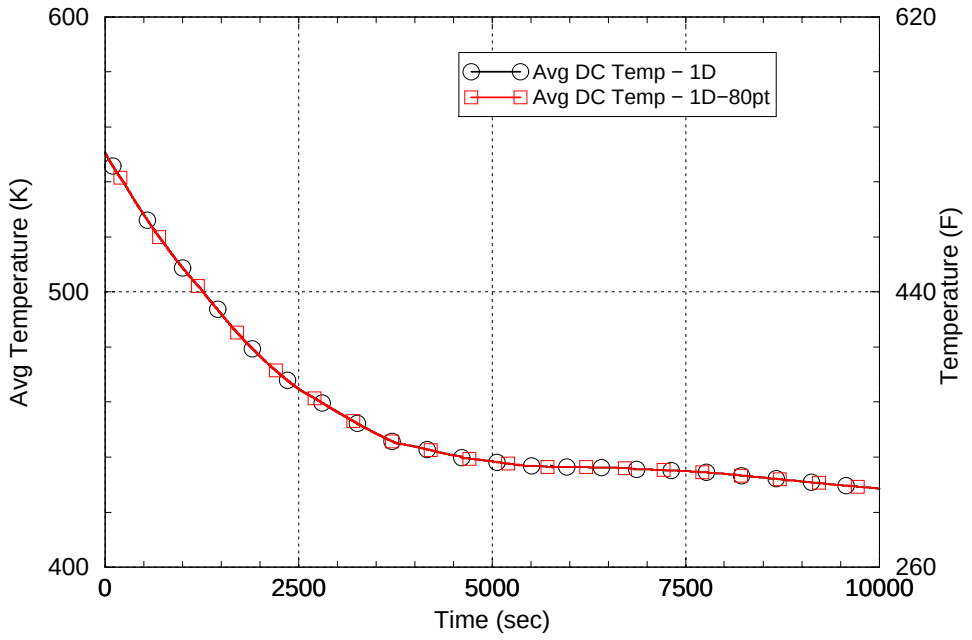

Figure 4-13: Case 19 Avg. Downcomer Temperature (1D vs 1D-80 Nodes)

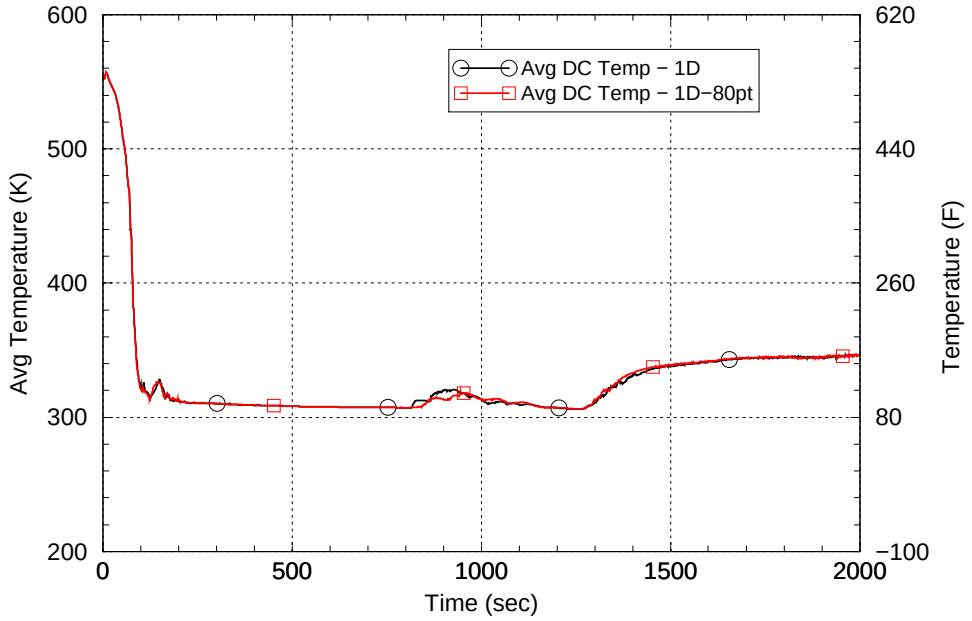

Figure 4-14: Case 40 Avg. Downcomer Temperature (1D vs 1D-80 Nodes)

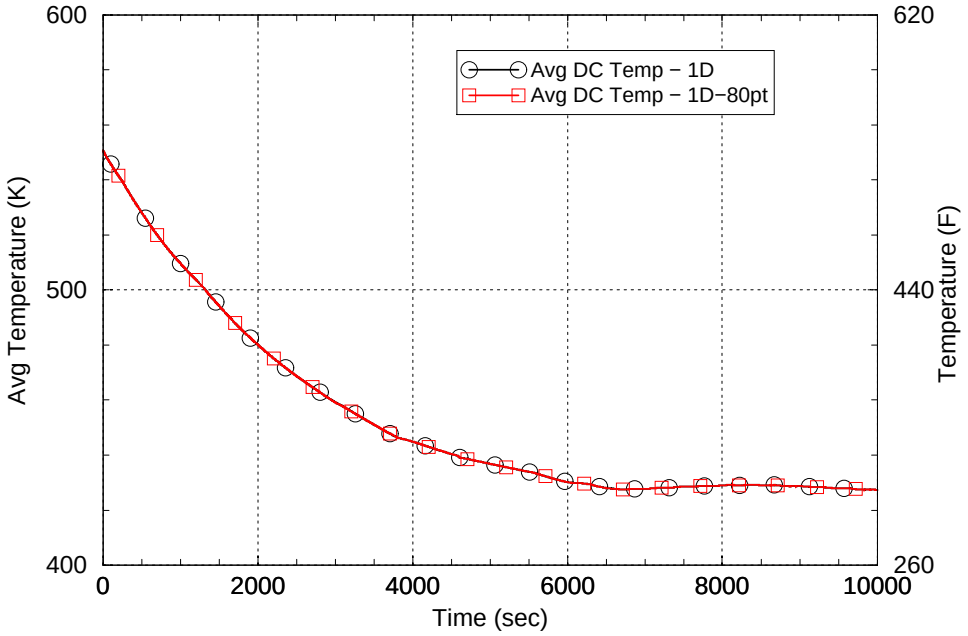

Figure 4-15: Case 52 Avg. Downcomer Temperature (1D vs 1D-80 Nodes)

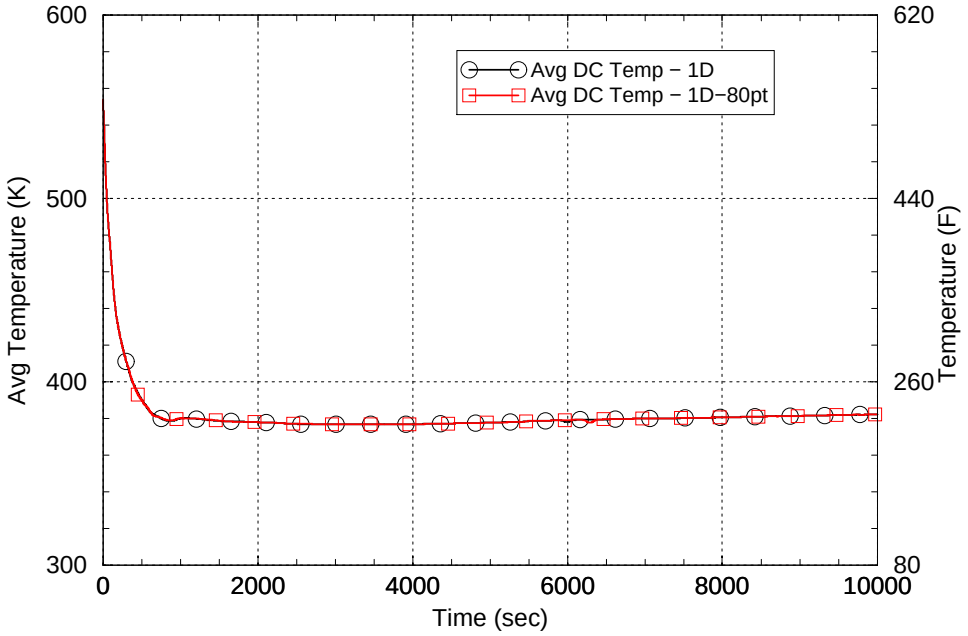

Figure 4-16: Case 54 Avg. Downcomer Temperature (1D vs 1D-80 Nodes)

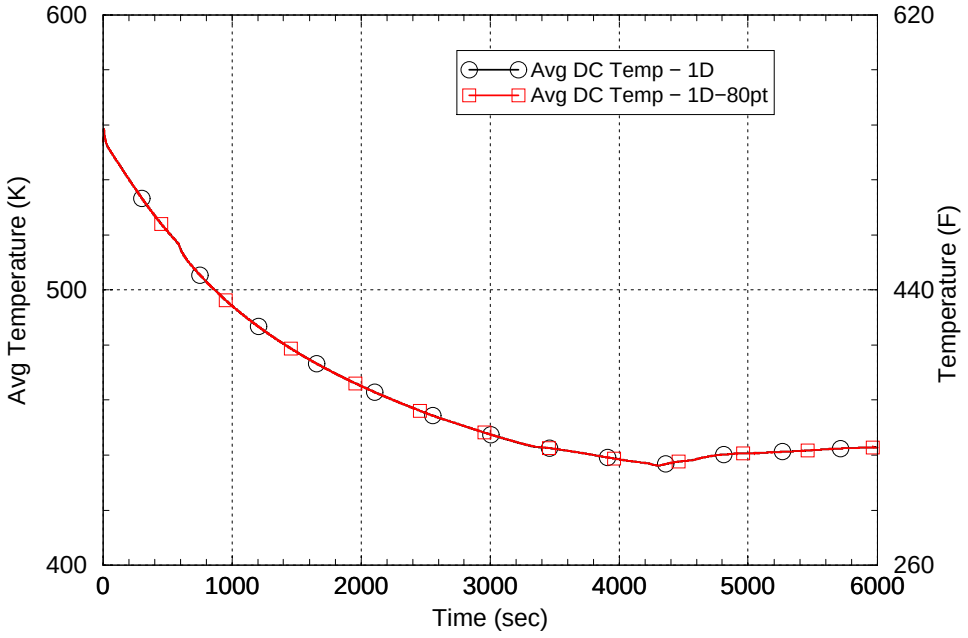

Figure 4-17: Case 55 Avg. Downcomer Temperature (1D vs 1D-80 Nodes)

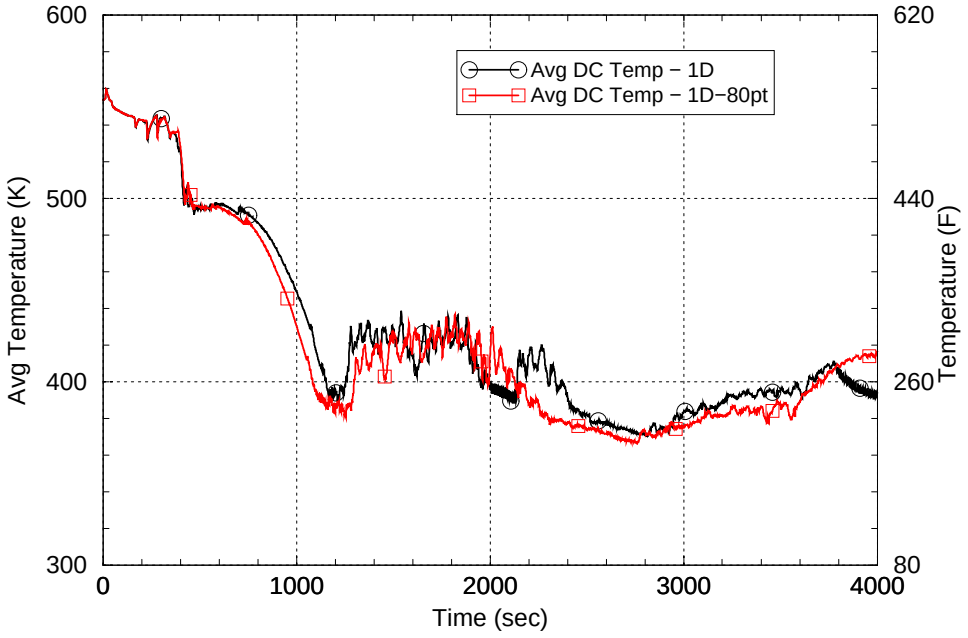

Figure 4-18: Case 58 Avg. Downcomer Temperature (1D vs 1D-80 Nodes)

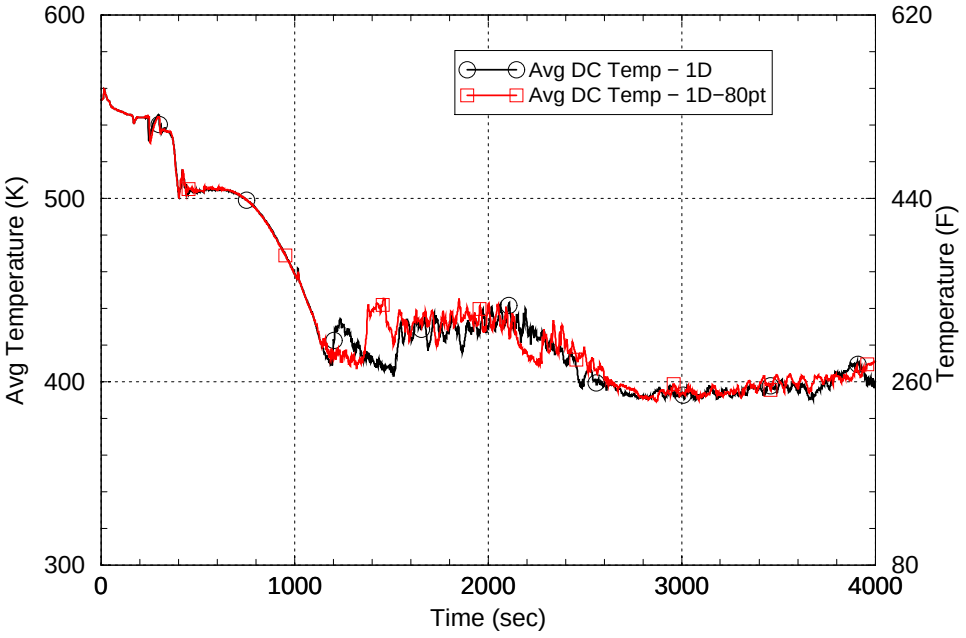

Figure 4-19: Case 59 Avg. Downcomer Temperature (1D vs 1D-80 Nodes)

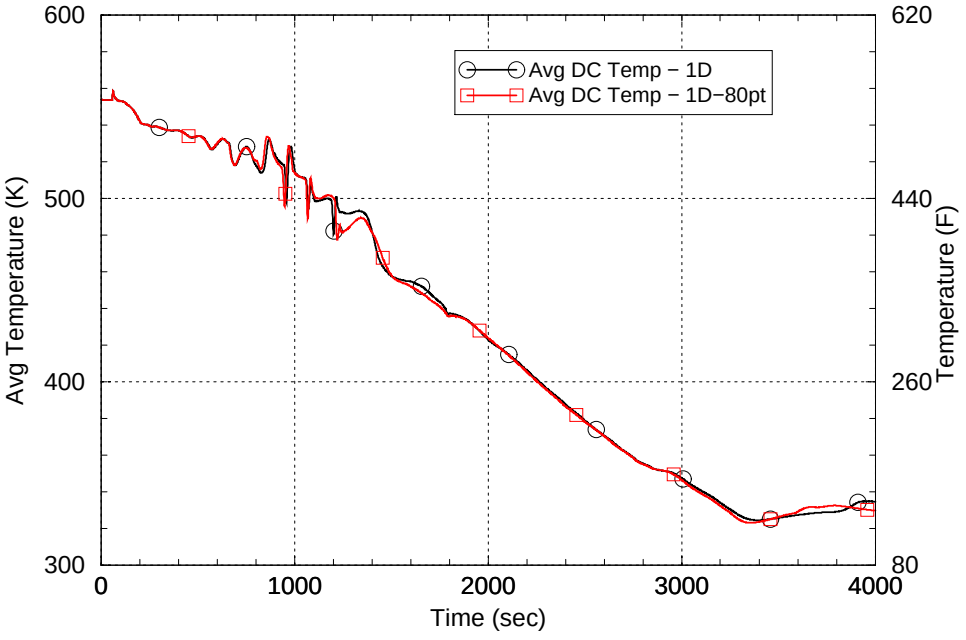

Figure 4-20: Case 60 Avg. Downcomer Temperature (1D vs 1D-80 Nodes)

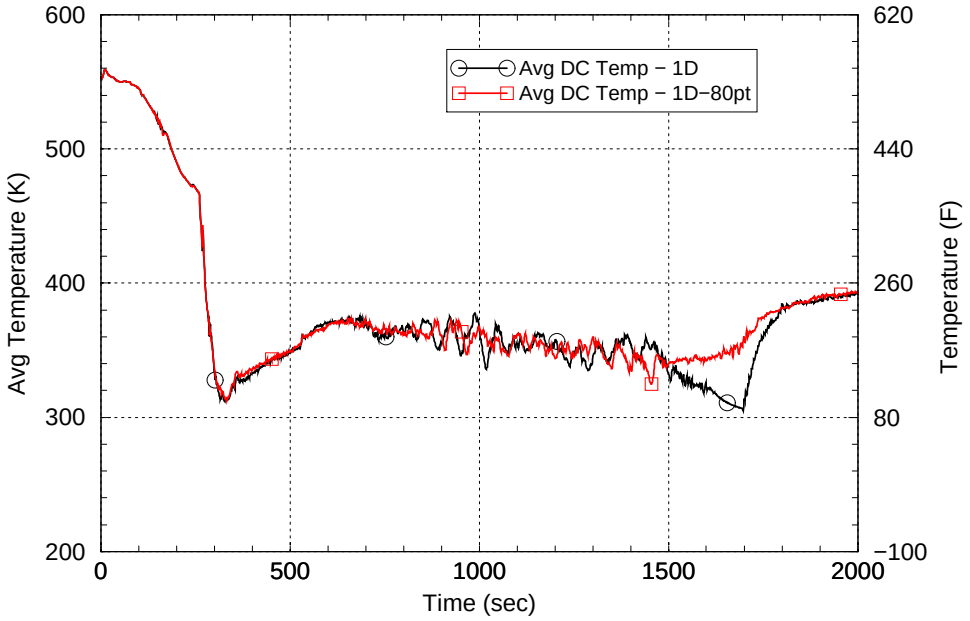

Figure 4-21: Case 62 Avg. Downcomer Temperature (1D vs 1D-80 Nodes)

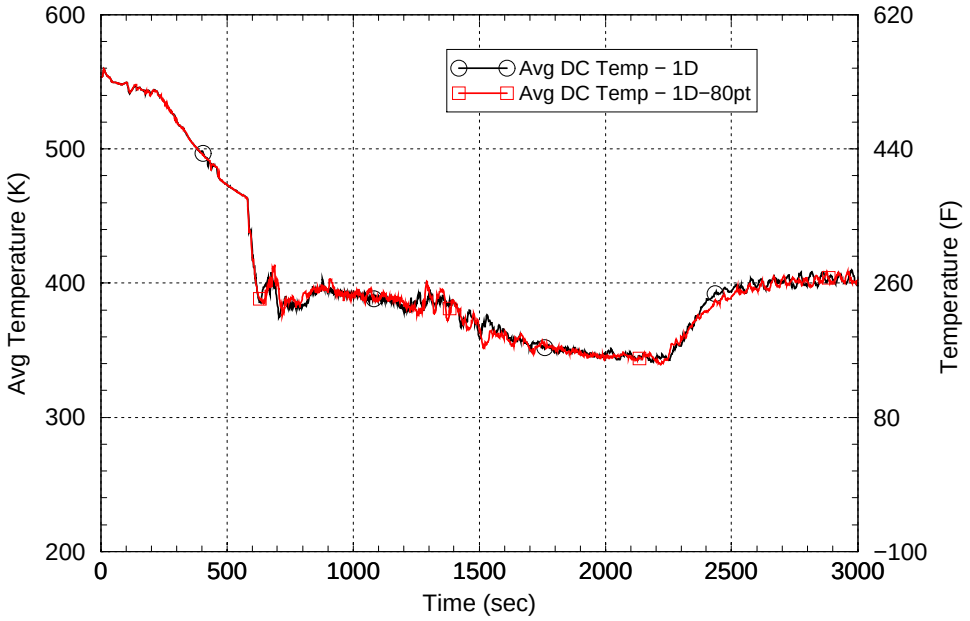

Figure 4-22: Case 63 Avg. Downcomer Temperature (1D vs 1D-80 Nodes)

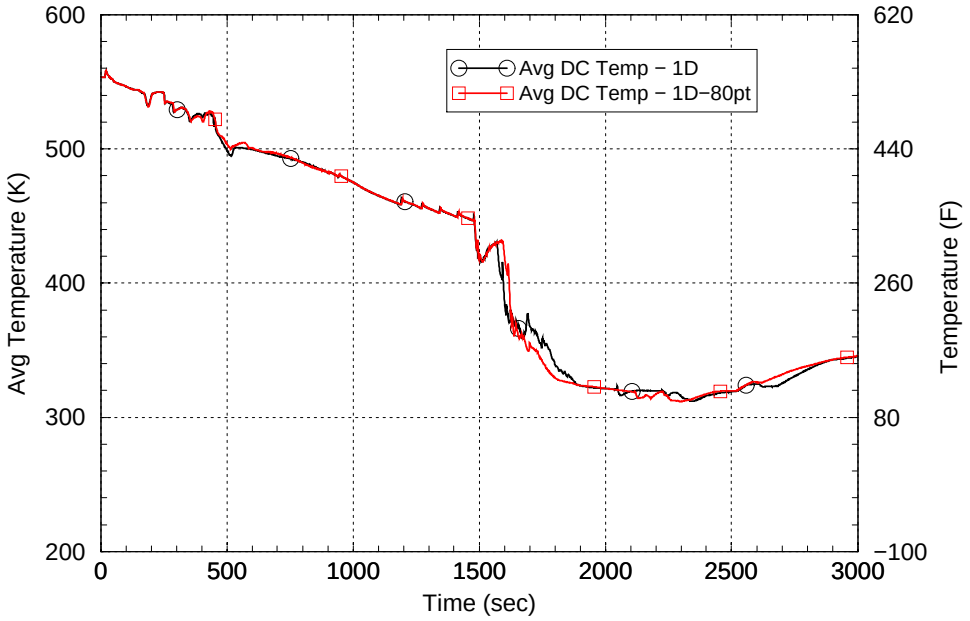

Figure 4-23: Case 64 Avg. Downcomer Temperature (1D vs 1D-80 Nodes)

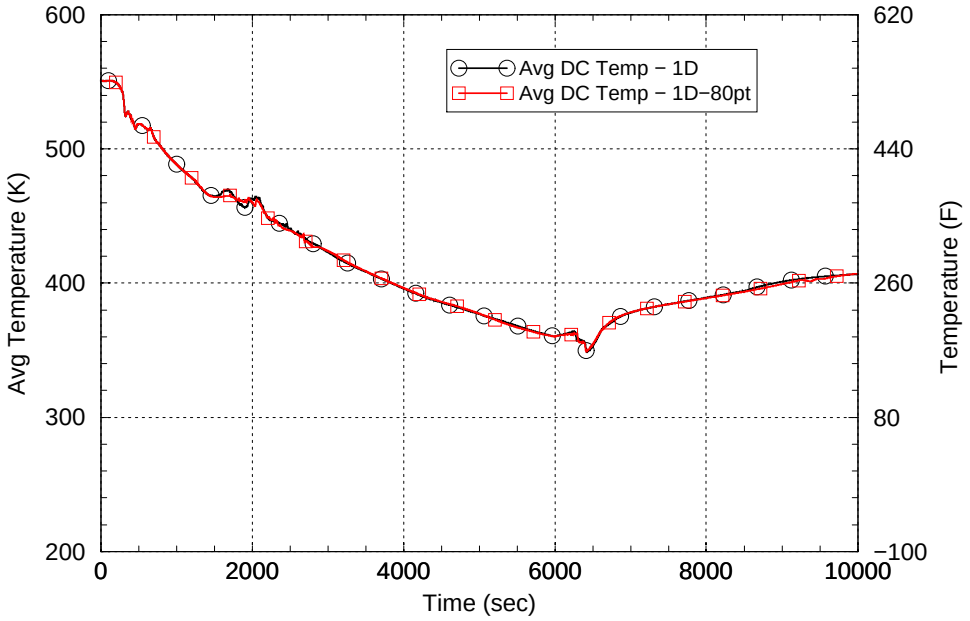

Figure 4-24: Case 65 Avg. Downcomer Temperature (1D vs 1D-80 Nodes)

4.3 Heat Transfer Coefficient Sensitivity Results

Figures 4-25 to 4-36 present a comparison of the downcomer fluid to wall heat transfer coefficient between Variations 9 and 10 listed in Table 2. Variation 9 utilizes a 1D downcomer model with 80 nodes in the vessel wall. Variation 10 is the same as Variation 9 except that the ORNL ANS Interphase (Petukhov) correlation with the Swanson-Catton multiplier is used. In both cases, the heat transfer coefficient results for the 10 second running average is used because the implementation of the Petukhov correlation in RELAP5/MOD3.2.2 gamma tends to produce noisy results. The 10 seconds running average results were used for the sensitivity studies in this case.

In general, the effect of the application of the Petukhov correlation with the Swanson-Catton multiplier is to increase the value of the downcomer fluid to wall heat transfer coefficient. In some of the smaller LOCAs, particularly the cold leg breaks, the value of the heat transfer coefficient in Variation 10 drops below the value computed in Variation 9. Case 64 is an instance where the Variation 10 value drops below the Variation 9 value for an extended period of time (600 to 1500 seconds after initiation). This difference is due to different predictions of the heat transfer mode that is occurring during this period. In the case of Variation 9, the dominant heat transfer mode is subcooled nucleate boiling (mode 3). In Variation 10, the dominant mode is single phase liquid convection with a subcooled wall and low void fractions (mode 2). Changing the heat transfer coefficient model causes differences in the system thermal hydraulics that are sufficient to cause differences in the heat transfer mode predictions and ultimately the heat transfer coefficient results.

It is instructive to look at the effect of the downcomer fluid to wall heat transfer coefficient on the prediction of downcomer fluid temperature and downcomer wall temperature. Using Case 64 as an example, the downcomer fluid temperature is significantly lower for Variation 10 compared to Variation 9 from 600 to 1500 seconds after initiation while the heat transfer coefficient is significantly lower. This trend is seen for all of the transients analyzed in Variations 9 and 10 (see plots in file avgDCTemp_1D_80pt_Petukhov.pdf and avgHTC_1D_80pt_Petukhov.pdf) where the reactor coolant pumps trip. For Cases 19, 52 and other cases where the reactor coolant pumps remain running, downcomer heat transfer is conduction limited and the differences in heat transfer coefficient have no effect. These observations are instructive because there is a perception that higher values of the heat transfer coefficients are worse from a pressurized thermal shock standpoint, which may not be true if the downcomer fluid temperature is also higher as a result.

Variations 11 and 12 listed in Table 2 are the same as variation 10 except for the application of a multiplier on the downcomer fluid to wall heat transfer coefficient value predicted by RELAP5. The average downcomer fluid temperature, system pressure and other system parameters are otherwise identical.

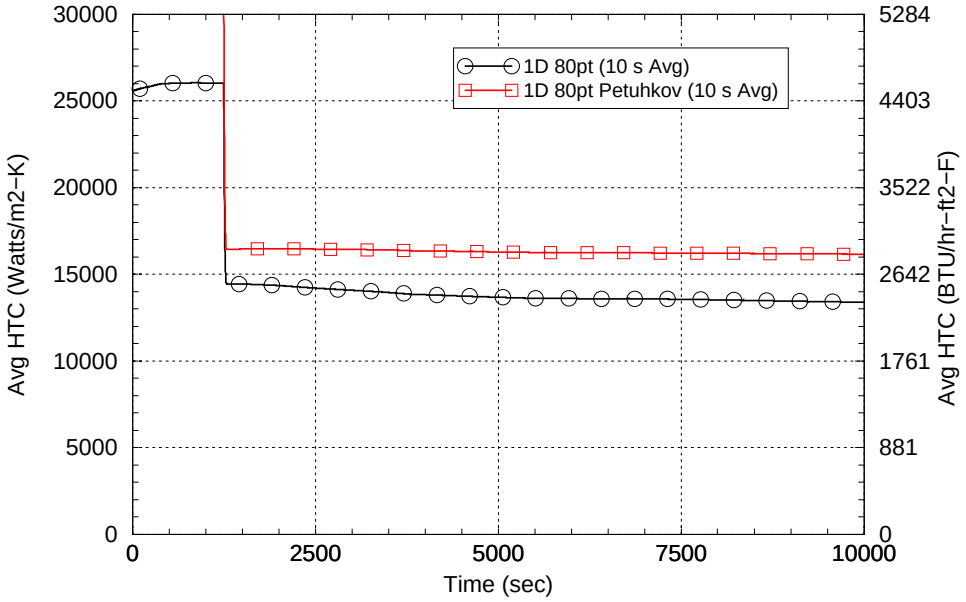

Figure 4-25: Case 19 Avg. HTC (1D-80 Nodes vs 1D-80 Nodes w Petukhov)

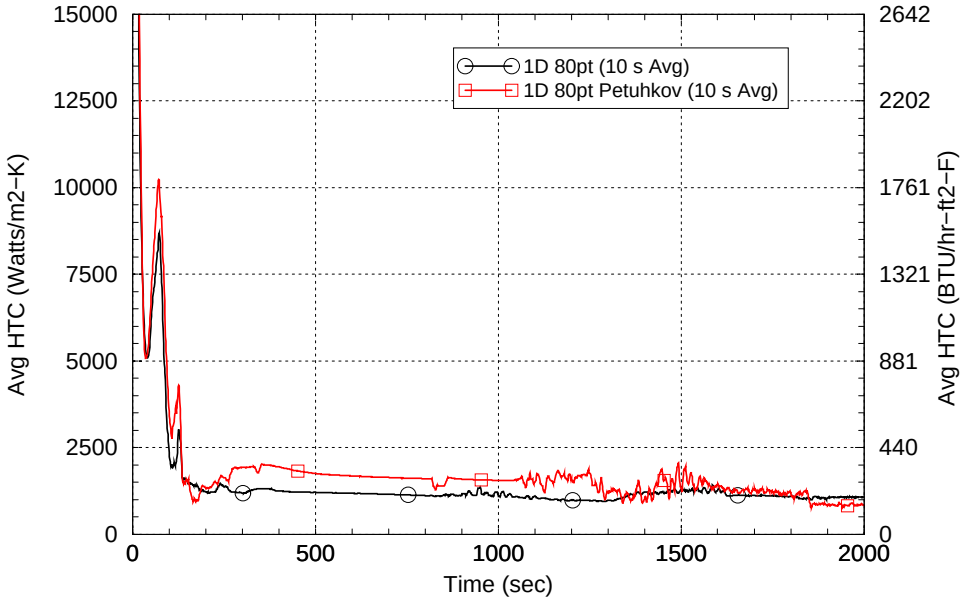

Figure 4-26: Case 40 Avg. HTC (1D-80 Nodes vs 1D-80 Nodes w Petukhov)

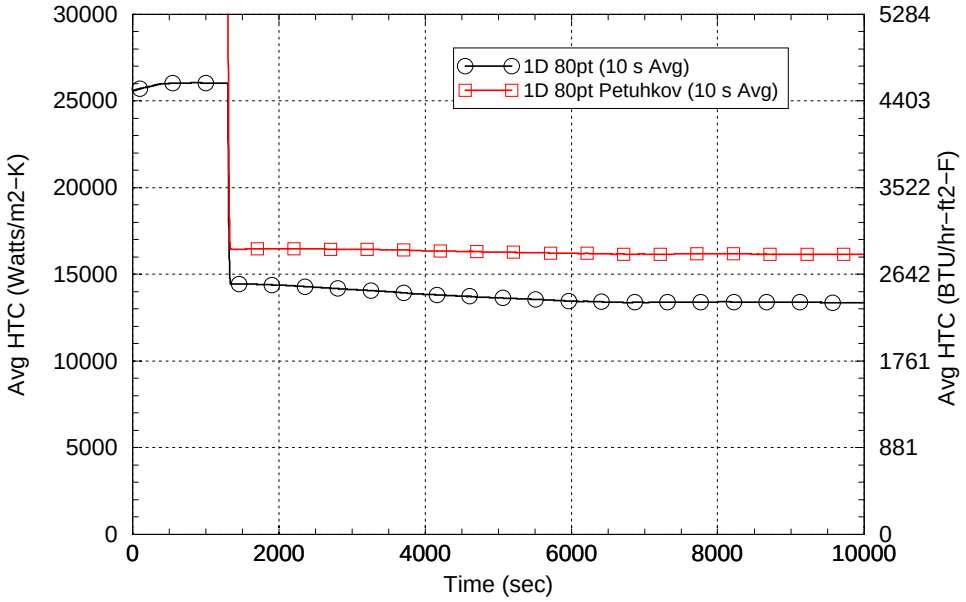

Figure 4-27: Case 52 Avg. Heat Transfer Coeff (1D-80 Nodes vs 1D-80 Nodes w Petukhov)

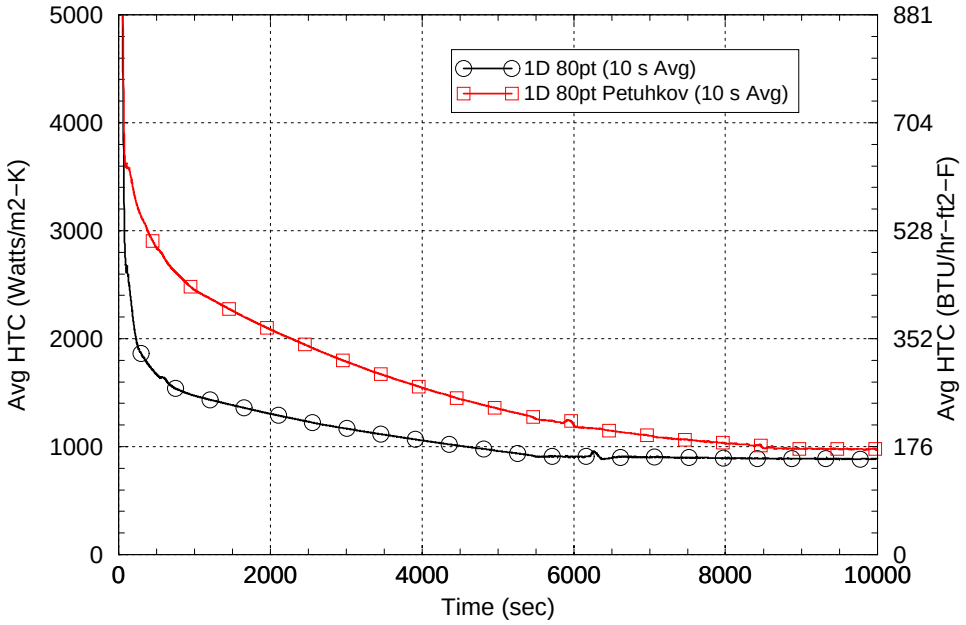

Figure 4-28: Case 54 Avg. HTC (1D-80 Nodes vs 1D-80 Nodes w Petukhov)

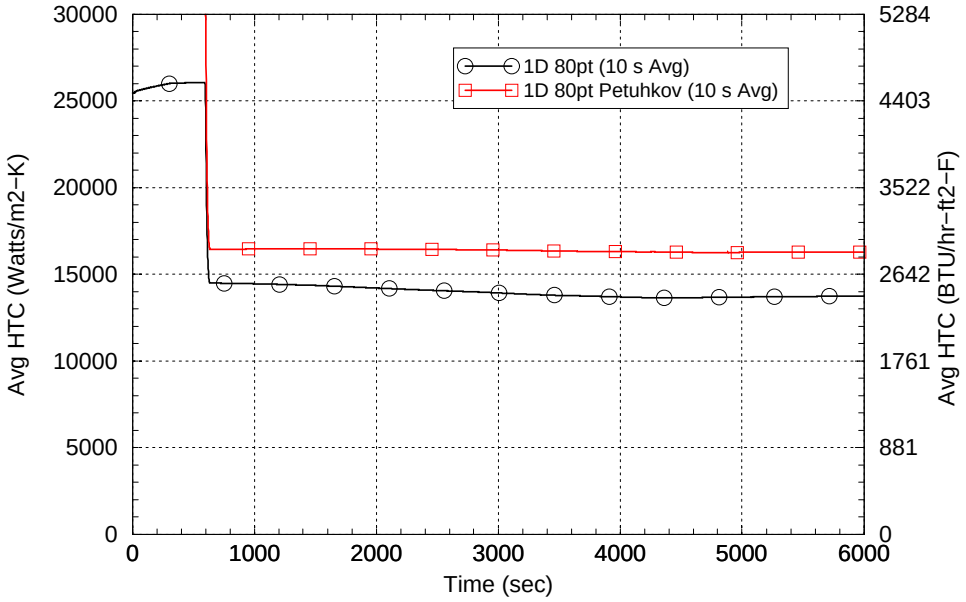

Figure 4-29: Case 55 Avg. HTC (1D-80 Nodes vs 1D-80 Nodes w Petukhov)

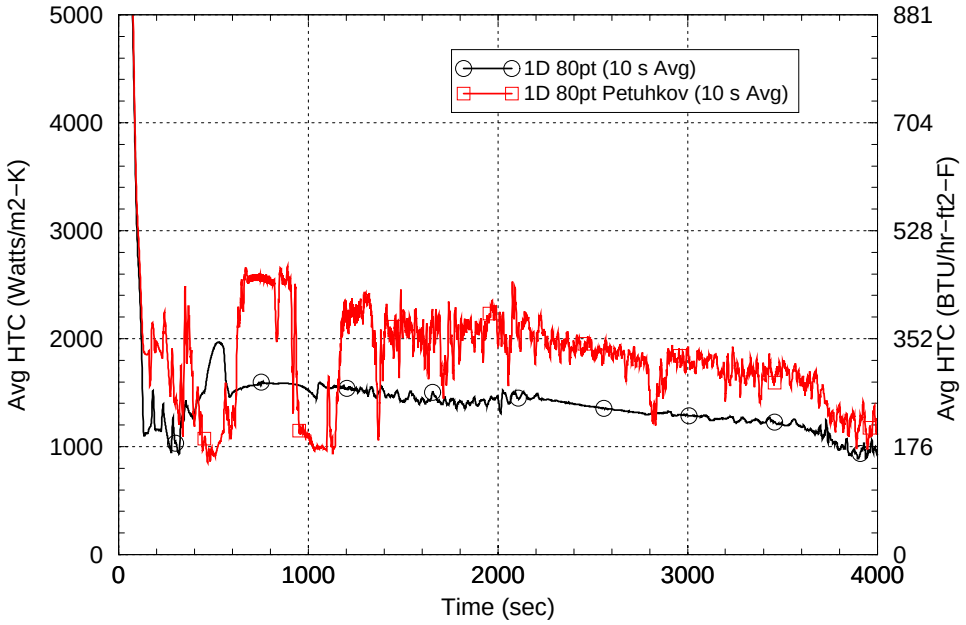

Figure 4-30: Case 58 Avg. HTC (1D-80 Nodes vs 1D-80 Nodes w Petukhov)

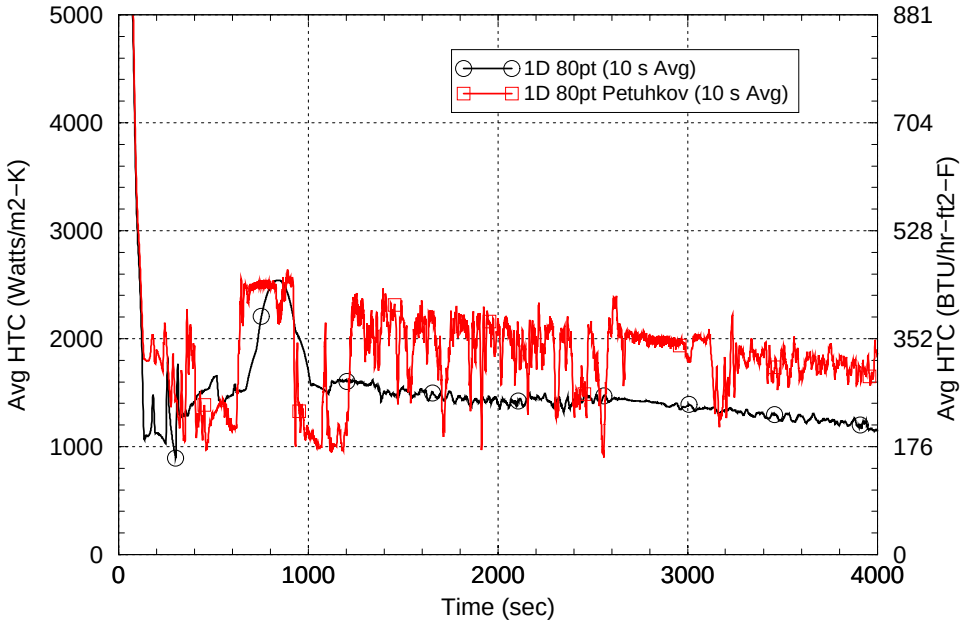

Figure 4-31: Case 59 Avg. HTC (1D-80 Nodes vs 1D-80 Nodes w Petukhov)

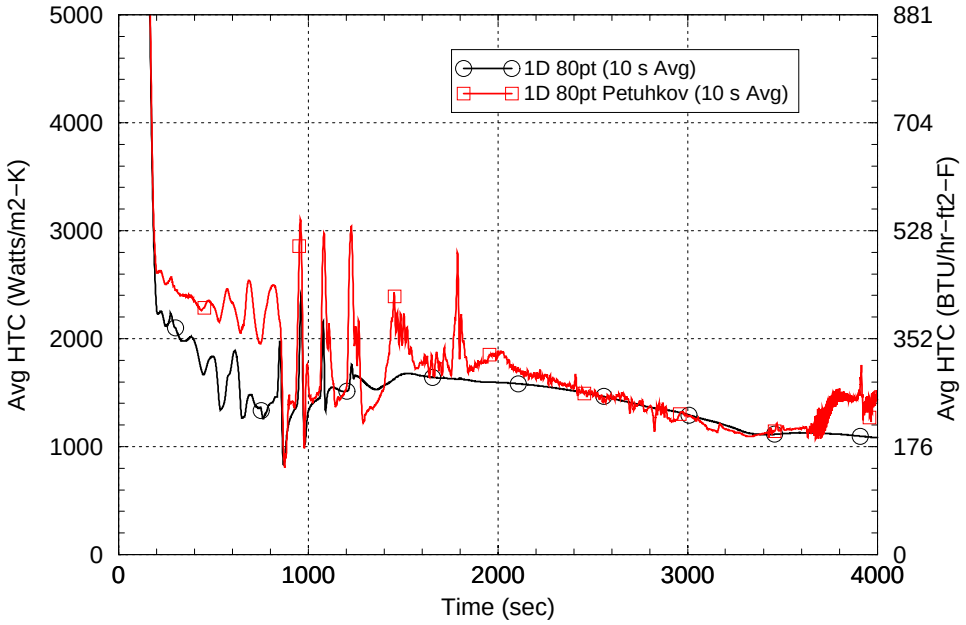

Figure 4-32: Case 60 Avg. HTC (1D-80 Nodes vs 1D-80 Nodes w Petukhov)

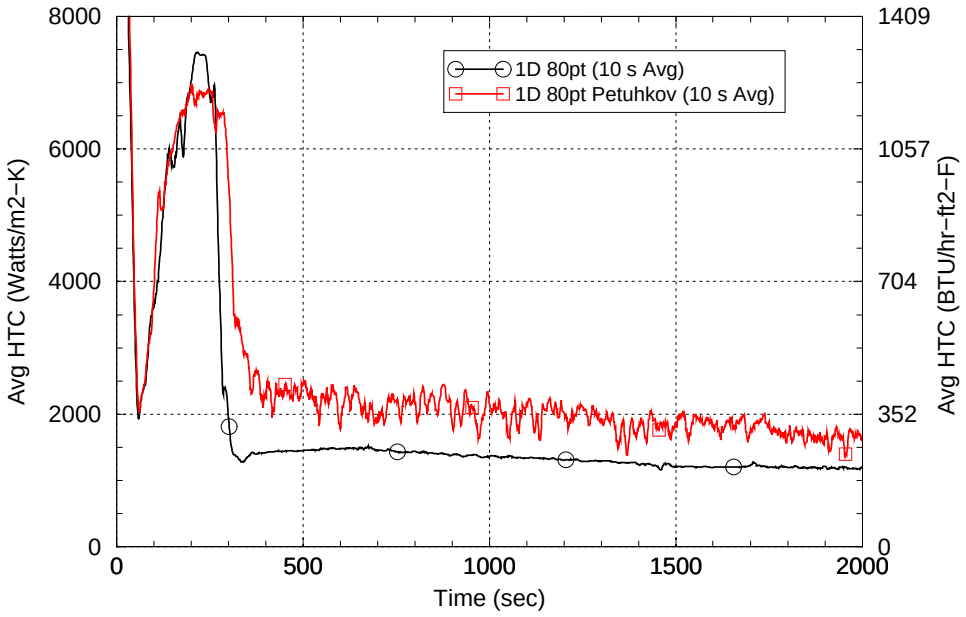

Figure 4-33: Case 62 Avg. HTC (1D-80 Nodes vs 1D-80 Nodes w Petukhov)

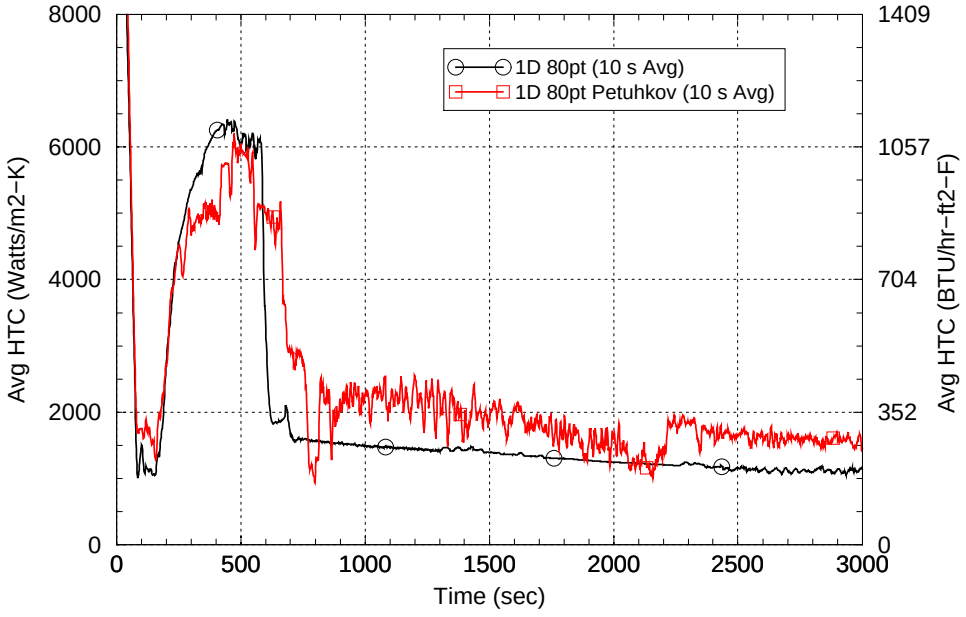

Figure 4-34: Case 63 Avg. HTC (1D-80 Nodes vs 1D-80 Nodes w Petukhov)

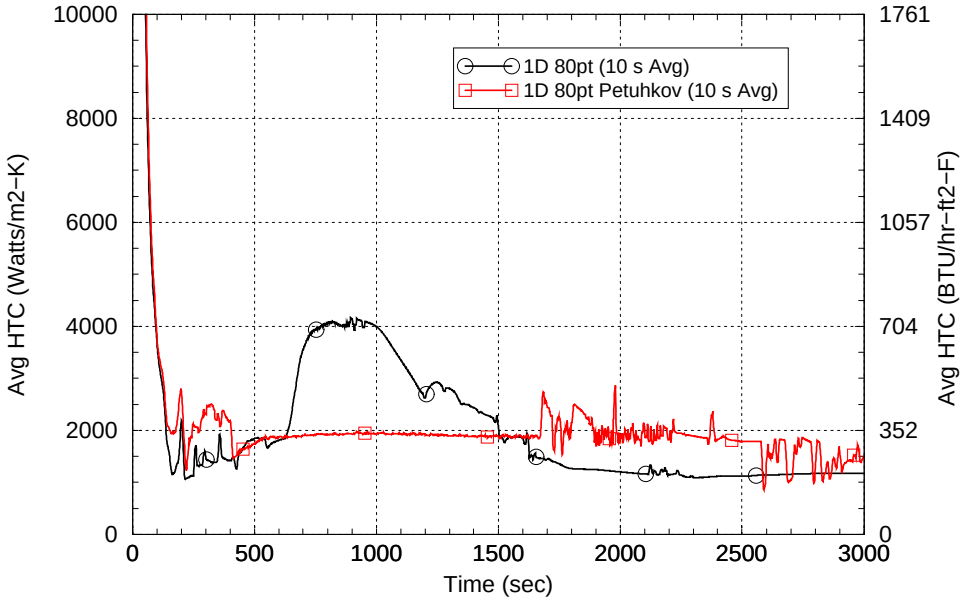

Figure 4-35: Case 64 Avg. HTC (1D-80 Nodes vs 1D-80 Nodes w Petukhov)

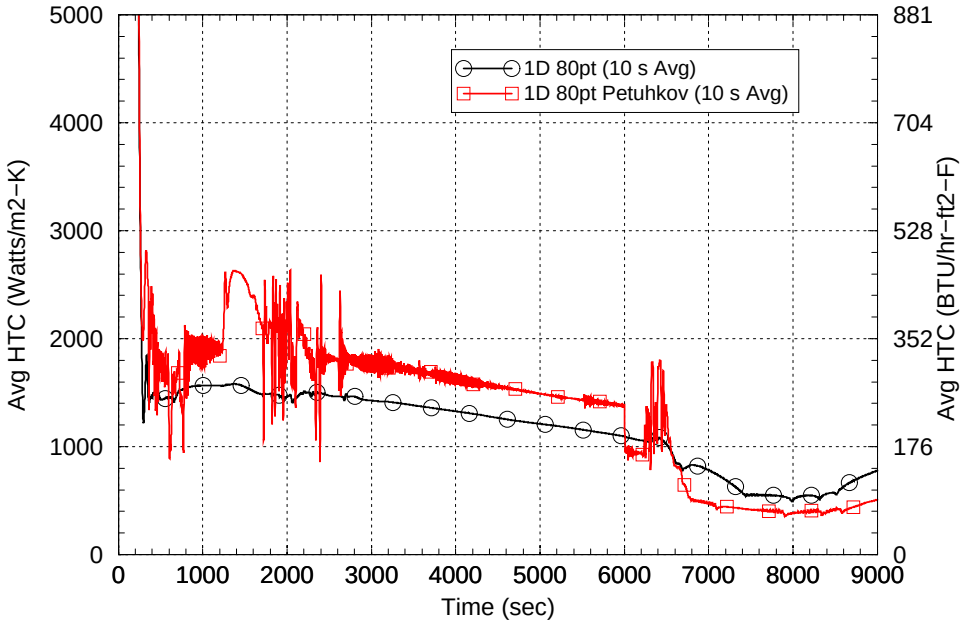

Figure 4-36: Case 65 Avg. HTC (1D-80 Nodes vs 1D-80 Nodes w Petukhov)

5.0 Conclusions

RELAP5 sensitivity cases were performed to determine the effect on the parameters of interest in computing the conditional probability of vessel failure using the Favor code as a result of various RELAP5 model changes. These parameters are the average downcomer fluid temperature, primary system pressure and downcomer fluid to wall heat transfer coefficient. The model changes evaluated are the use of a 1D downcomer model relative to a 2D downcomer model, the use of 80 nodes in the vessel wall relative to 8 nodes, and the application of the Swanson-Catton multiplier on the ORNL ANS Interphase model which uses the Petukhov heat transfer correlation.

From a thermal hydraulic perspective, the cases where the greatest differences were found are for primary system LOCAs in the 5.08 cm (2 in) to 10.16 cm (4 in) range. Cold leg breaks generally show the most differences because of relatively unstable flow characteristics compared to hot leg breaks. Little difference is seen in cases where the primary system remains intact such as stuck-open secondary side relief valves or main steam line breaks.

Dickson summarized the results of determining the frequency of crack initiation (FCI) and the through wall crack frequency (TWCF) using the Favor probabilistic fracture mechanics code for the 12 variations (Table 2) on the 12 transients (Table 1) discussed in this report (Ref. 5 - see the References directory on the attached CDROM). The ultimate objective of these sensitivity cases is to determine the effect of the RELAP5 model changes on the results on the FCI and TWCF predictions, so it is appropriate to briefly review these results.

Basically, Dickson concluded that the impact of the RELAP5 model changes on the overall FCI and TWCF results for any of the 12 variations is small. The largest changes were seen from using the 1D downcomer model instead on the 2D model, changing the downcomer fluid to wall heat transfer coefficient by a factor of 0.7 and 1.3, and application of the ORNL ANS Interphase (Petukhov) model with the Swanson-Catton multiplier (Variation 10). Changing the downcomer model from 2D to 1D decreased the overall FCI and TWCF by 57% and 50%, respectively. Increasing the downcomer fluid to wall heat transfer coefficient by a factor of 1.3 increased the FCI and TWCF by a factor of 2.41 and 2.76, respectively. Conversely, decreasing the heat transfer coefficient by a factor of 0.7 decreases the FCI and TWCF by a factor of 77% and 67%, respectively. The application of the Petukhov model with the Swanson-Catton multiplier increased the FCI and TWCF by a factor of 3.93 and 1.90, respectively. The impact of the running average sensitivity studies and the changing number of nodes from 8 to 80 had a small impact on the FCI and TWCF results. Dickson noted that the risk profile, that is the relative contribution of each transient to the total risk for a given variation, can change significantly depending on the variation analyzed.

6.0 References

1. U.S. Nuclear Regulatory Commission, *RELAP5/MOD3 Code Manual, Volume 1: Code Structure, System Models and Solution Methods*, NUREG/CR-5535, Volume 1, June 1999
2. Swanson, L.W. and Catton, I., *Enhanced Heat Transfer Due to Secondary Flows in Mixed Turbulent Convection,* Journal of Heat Transfer, Vol. 109, pp. 943-946, November 1987
3. Shumway, Rex, *Documentation of RELAP5 Parallel Plate Heat Transfer Model*, 17 June 2004 (See the Petukhov-Catton.pdf file in the Reference directory on the attached CDROM)
4. Arcieri, W.C., Beaton, R.M., Fletcher, C.D. and Bessette, D.E., *RELAP5 Thermal Hydraulic Analysis to Support PTS Evaluations for the Oconee-1, Beaver Valley-1, and Palisades Nuclear Power Plants*, NUREG/CR-6858, completed September 2004
5. Dickson, Terry L., *PFM Sensitivity Analysis for TH Perturbations*, Report transmitted to Mark Kirk of the NRC via. Email on 6/7/04.